Diagnosis of virus infection in orchid plants with high-resolution optical coherence tomography

Tzu H. Chow
Khay M. Tan
Beng K. Ng
Sirajudeen G. Razul
Chia M. Tay
Nanyang Technological University
School of Electrical and Electronic Engineering
Photonics Research Centre
Singapore 639798, Singapore

Tet F. Chia
National Institute of Education
Natural Sciences and Science Education
1 Nanyang Walk
NIE7-03-95
Singapore 637616, Singapore

Wee T. Poh
Changi General Hospital
Histology Laboratory
2 Simei Street 3
Singapore 529889, Singapore

Abstract. This work investigates the use of optical coherence tomography (OCT) to identify virus infection in orchid plants. Besides revealing the cross-sectional structure of orchid leaves, highly scattering upper leaf epidermides are detected with OCT for virus-infected plants. This distinct feature is not observable under histological examination of the leaf samples. Furthermore, the leaf epidermides of stressed but healthy plants, which exhibit similar visual symptoms as virus-infected plants, are not highly scattering and are similar to those of healthy plants. The results suggest that virus-infected orchid plants can be accurately identified by imaging the epidermal layers of their leaves with OCT. The OCT modality is suitable for fast, nondestructive diagnosis of orchid virus infection, which may potentially lead to significant cost savings and better control of the spread of viruses in the orchid industry. © *2009 Society of Photo-Optical Instrumentation Engineers.* [DOI: 10.1117/1.3066900]

Keywords: optical coherence tomography; plant imaging; virus; scattering.

Paper 08292R received Aug. 19, 2008; revised manuscript received Nov. 11, 2008; accepted for publication Nov. 15, 2008; published online Jan. 20, 2009.

1 Introduction

Orchid culture and export is an important business in many countries. Singapore, for example, exported S$26 million worth of fresh orchids, orchid plants, and cuttings in 2006.[1] Viral diseases are a major problem in the orchid industry due to their detrimental effects on the quality of the flowers and plants, which directly affects their exportability. Two most prevalent and economically important orchid viruses are the Cymbidium Mosaic Virus (CymMV) and the Odontoglossum Ringspot Virus (ORSV).[2] They are known to cause chlorosis and deformation in the leaves, color break in the flowers, and a reduction in flower yield. The main source of virus transmission is the horticultural tools used to divide plants and harvest flowers. There is presently no cure once a plant is infected, and the only effective control measure is to isolate and destroy the infected plants.

The current gold standard test for detecting virus infection in orchid plants is the enzyme-linked immunosorbent assay (ELISA),[3] a serological detection technique that requires plant samples to be sent to a commercial laboratory. Another method that utilizes polymerase chain reaction (PCR) to amplify the viral nucleic acids for electrophoresis analysis is reported to be more sensitive and reliable than ELISA.[4] However, both methods have to be performed in the laboratory, are time consuming, and destructive. Moreover, decision on selecting orchid plants for virus infection tests is mainly based on visually obvious color breaks in flowers or chlorosis in leaves. This method of visual inspection has several limitations. First, orchid plants suffering from virus infection may not show visible symptoms. Furthermore, factors such as abnormal nutrition and environmental conditions can also produce virus-like symptoms. Last, it is often too late when visual symptoms appear, as this usually implies that the plant is already badly infected.

The efficient control of orchid virus diseases requires rapid and accurate diagnosis. Optical coherence tomography (OCT) is a noninvasive, low coherence imaging method that can potentially fulfill the need for a fast and nondestructive diagnostic tool. The OCT technique has generated numerous biomedical applications, most notably in the field of ophthalmology[5,6] and dermatology.[7] Cross sectional OCT images are obtained by interferometrically detecting the backreflected or backscattered light from the internal microstructures of biological entities. Interferometric detection of the returned light ensures that extremely small reflections corresponding to small index mismatches can be measured. The imaging depth of OCT is primarily limited by optical absorption and scattering, and morphologic features as deep as *3* mm can be imaged in tissues. With down to micrometer axial resolution, the technique is capable of producing high resolution images of tissue structure beneath the surface layer that is comparable to histology,[8] and has potential applications in the *in-situ*, real-time diagnosis of early neoplasia. More recently, OCT has also been used in the area of botany to visualize the inner structures of botanical subjects[9,10] and to study the early physiological changes in plants suffering from a pathogen attack.[11]

Address all correspondence to: T. H. Chow, School of Electrical and Electronic Engineering, Photonics Research Centre, Nanyang Technological University, Photonics Lab 1, 50 Nanyang Avenue, S1-B3a-08, Singapore 639798. Tel: 67906319; Fax: 67904161; E-mail: chow0035@ntu.edu.sg.

1083-3668/2009/14(1)/014006/6/$25.00 © 2009 SPIE

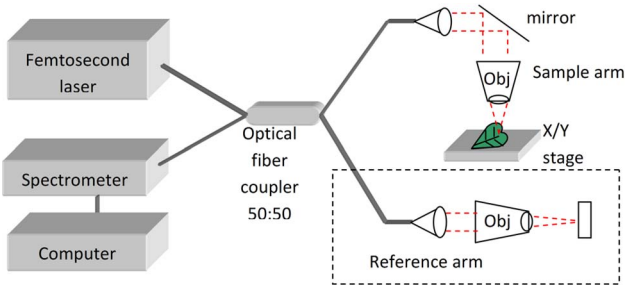

Fig. 1 Experimental setup of the FD-OCT system used in this study.

In this work, we investigate the use of a high resolution OCT method to nondestructively examine leaf samples from both healthy and virus-infected orchid plants. This study focuses on CymMV-infected plants, since its incidence is significantly higher than those of the ORSV type.[2] The OCT images of the leaf samples were compared with histological analysis and correlated to the standard ELISA test. The OCT images of leaf samples from stressed but healthy plants exhibiting virus-like visual symptoms were also obtained for comparison.

2 Materials and Methods

2.1 *Optical Coherence Tomography*

A Fourier domain OCT (FD-OCT) system[12] was set up in this work to achieve high resolution OCT imaging. The schematic diagram of our FD-OCT system is shown in Fig. 1. The light source used in the system is an Integral OCT femtosecond laser (Femtolasers Produktions GmbH, Vienna, Austria) with a center wavelength of 820 nm and an optical bandwidth of about 120 nm. Identical microscope objective lenses (NA =0.3) were placed in the sample and reference arms to mitigate dispersion mismatch in the two arms. The laser light is coupled into a 2×2 fiber coupler, which splits it equally into the reference and sample arms. Light reflected from the reference and sample arms is combined in the interferometer and measured in the frequency domain using a spectrometer (HR4000, Ocean Optics, Dunedin, Florida). The original optical spectrum is modulated at a frequency directly proportional to the optical path length between the reference mirror and the sample. The spatial reflectance profile of the tissue is obtained from an inverse Fourier transform of the optical spectrum.

The axial resolution of the OCT setup was measured to be 4 μm in free space. The lateral resolution was 9 μm, as determined with a United States Air Force target card. To minimize dispersion effects caused by additional optics (which will worsen the axial resolution), the beam in the sample arm was not expanded after the collimation lens to fill the back aperture of the objective lens. As a result, the measured lateral resolution was poorer than the theoretical resolution of 1.5 μm. A signal-to-noise ratio of 93 dB was achieved with this setup. The scan rate was about 1 A-line/s and was limited by the acquisition time of the spectrometer and the signal processing time for data scaling and Fourier transforms. The power delivered to the leaf sample was about 5 mW, which, together with the objective lens, gave an irradiance that was lower than the damage threshold of plant leaves.[13] Furthermore, the laser pulse width was broadened significantly by dispersion after passing through various optical components. Consequently, the peak power was also not sufficient to damage the leaf samples.

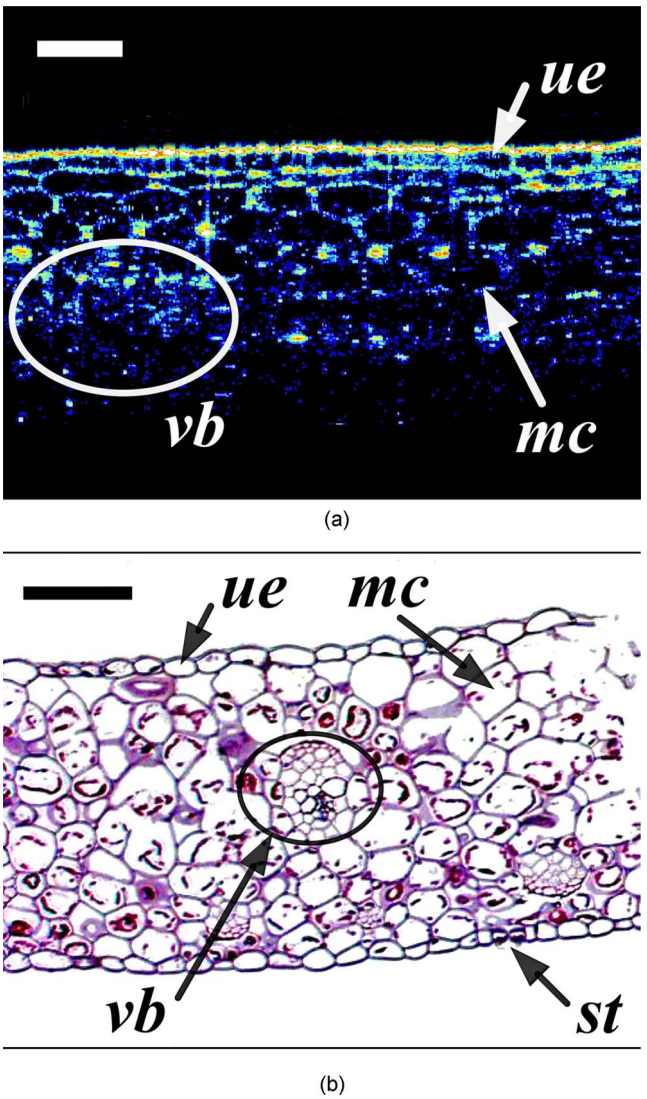

Fig. 2 Comparison between the (a) OCT image and (b) histological section of an orchid leaf sample. Scale bar corresponds to 100 μm. ue—upper epidermis, vb—vascular bundle, st—stoma, and mc—mesophyll cell.

2.2 *Plant Materials*

Leaf samples from Oncidium orchid plants were used in this study. Leaf samples with differing symptoms were collected from both healthy and CymMV-infected plants. The main source of infection in the CymMV-infected plants is through the horticultural tools used in dividing plants and harvesting flowers. The plants were infected with CymMV for up to 6 months. These leaf samples were first imaged using our FD-OCT system immediately after they were harvested to obtain cross sectional OCT images. After OCT imaging, part of the leaf samples was subjected to standard histological preparation (fixation, sectioning, and haematoxylin-eosin staining).

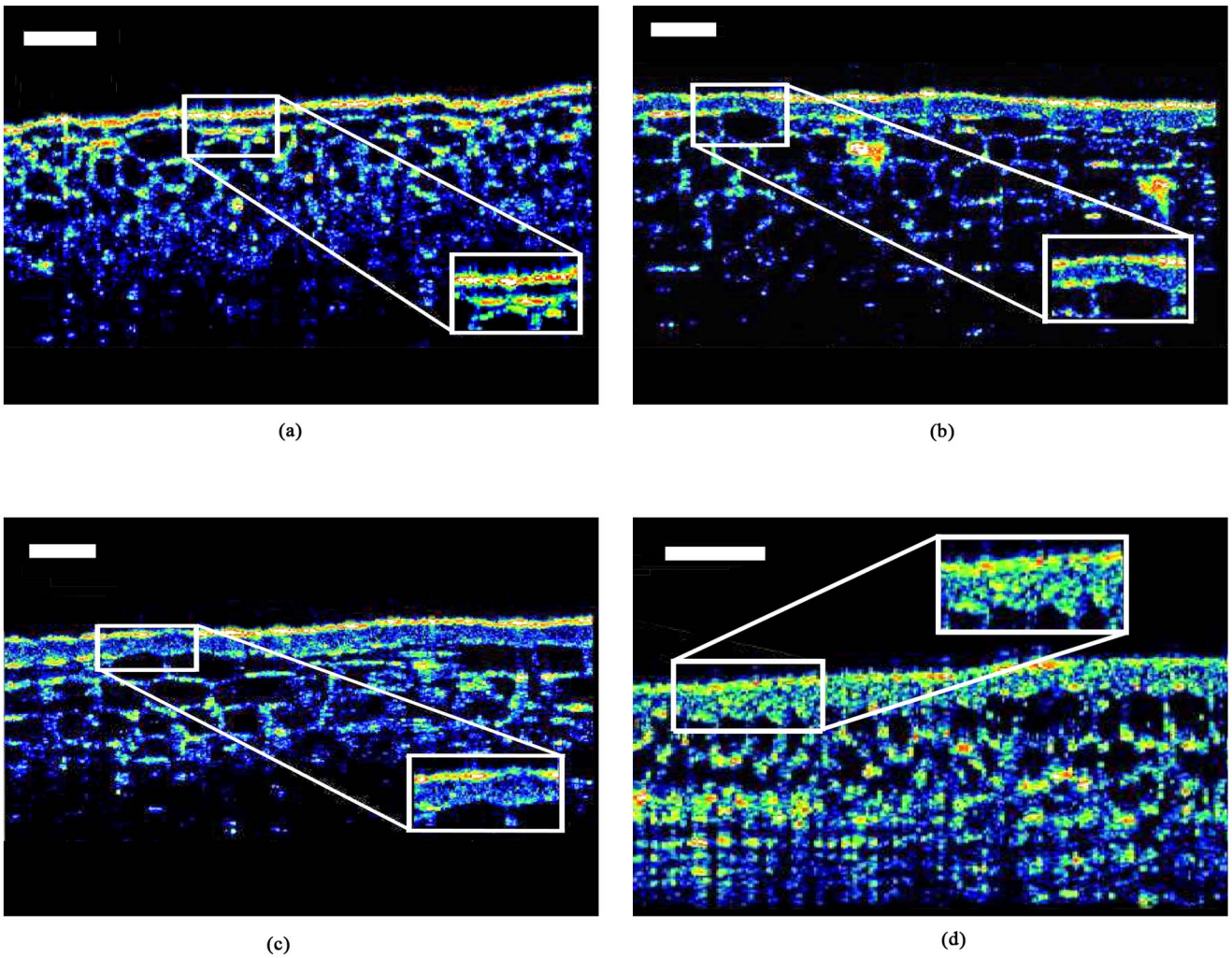

Fig. 3 OCT images of (a) a healthy young leaf, (b) a virus-infected leaf with chlorosis, (c) a virus-infected leaf without visible symptoms, and (d) a small young leaf with virus infection but no visible symptoms. Inset shows the magnified view of the upper epidermal layers of the leaf samples. Scale bar corresponds to 100 μm.

Some of the leaf samples underwent cryohistology to examine their optical properties without staining. The sections were then examined under a bright-field or phase-contrast microscope. The remaining leaf samples were sent for ELISA tests to positively identify virus-infected samples. We note that ELISA tests are sensitive enough to detect the presence of virus due to the high-titer nature of the CymMV in Oncidium orchids.[14–16]

3 Results

3.1 *Optical Coherence Tomography Analysis*

We first compare the OCT and bright-field histological images of a leaf sample from a healthy plant in Fig. 2. The OCT tomogram in Fig. 2(a) is a raw false-color image depicting the interferometrically detected optical intensity backscattered from different depths in a leaf sample. This backscattered intensity is associated with the differences in the refractive index between the cellular components and its surrounding medium in the plant tissue. The axial depth from the surface of the leaf sample is corrected using the average refractive index of plant tissues.[17]

Comparing the histological section of the leaf sample in Fig. 2(b), the upper epidermis, vascular bundle, and mesophyll cells are clearly evident in the OCT image. The distinctive horizontally elongated shape of epidermal cells and the more rounded shape of mesophyll cells are readily visible in the OCT image. The nuclei of the plant cells are barely discernible due to the resolution limits of the system. It can also be seen that the OCT signal is reduced with increasing depth into the leaf sample. An imaging optical depth of approximately 400 μm was achieved with the OCT system. As the leaf contains mostly water, an average refractive index of 1.33 was assumed, which results in a physical penetration depth of approximately 300 μm in the leaf. The limited measurement depth is attributed to the attenuation of the incident light via scattering in the plant tissue[18] and the sensitivity of the spectrometer.

We next compare the OCT images of leaf samples from both healthy and virus-infected plants in Fig. 3. Three

CymMV-infected leaf samples with differing symptoms were imaged with the OCT system. One of the virus-infected leaf samples has visible chlorosis, while the remaining samples have no visible symptoms, with one of them being a small young leaf. ELISA tests performed on these samples confirmed that they are infected with CymMV. The ELISA tests yielded positive CymMV infection with results of approximately 104-μg/g fresh weight for all three leaf samples.

The OCT images in Fig. 3 clearly revealed the epidermal layer and the underlying mesophyll cells in all the leaf samples. It is noted that the mesophyll cells in two of the virus-infected samples [Figs. 3(b) and 3(c)] are larger compared to those of the healthy sample. This can be explained by the larger size of the two virus-infected leaf samples in Figs. 3(b) and 3(c) compared to the healthy leaf sample. The region beneath the epidermal layer of the young leaf sample in Fig. 3(d) appears to be highly scattering, although this is not seen in the OCT images of other virus-infected young leaf samples. The origin of the highly scattering region throughout the young leaf sample is presently unclear, but it could be due to structural damage in the mesophyll cells as a result of the virus infection.

A clear difference between the OCT images of healthy and virus-infected leaf samples becomes apparent when we examine the epidermal layer. The epidermal layers of virus-infected samples are found to be highly scattering compared to that of a healthy sample. In particular, the horizontally elongated structure of the epidermal cells is no longer visible in the virus-infected leaf samples. Optical sections from the bottom surface of the leaf samples were also obtained with the OCT system. To verify the results, we imaged at least ten other healthy leaves (both young and matured) and virus-infected leaves that are visually symptom-free. The OCT images of all the leaf samples consistently showed a highly scattering epidermal layer in virus-infected leaf samples and a clear epidermal layer in healthy leaf samples.

As a quantitative measure, the average intensity value of the epidermis (excluding cell walls) in the OCT images was used to compare between the healthy and virus-infected leaves. This value is proportional to the intensity of the incident light and the reflectivity of the tissue components in the epidermis. The average intensity value over five healthy samples is 0.16 ± 0.09 (arbitrary units). By contrast, this value is 0.38 ± 0.22 for the five virus-infected samples. The average intensity values in the epidermis of healthy leaves are close to the measurement noise floor of 0.15, indicating that there is little or no scattering in the volume of healthy epidermal cells. The virus-infected samples have significantly larger average intensity values due to increased scattering in the epidermal cell volumes.

Abnormal nutrition and environmental conditions such as nutritional imbalance, excess salts, high light intensity, and genetic disorders can result in virus-like symptoms on orchid plants. A stressed plant can easily be mistaken to be virus-infected with just visual inspection. To investigate if stressed plants without virus infection exhibit the same high scattering feature in their leaves as virus-infected plants, we imaged leaf samples of several stressed plants that suffered from a lack of water over a prolong period. Figure 4 shows the typical OCT image of leaf samples from stressed plants without virus infection. The optical sections of these leaf samples are found to be similar to those of healthy leaves in Fig. 3(a). The stressed leaf samples did not have the highly scattering epidermal layer observed in the OCT images of virus-infected samples.

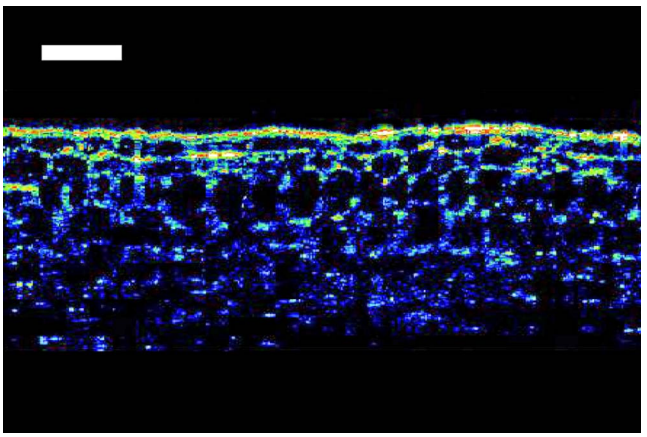

Fig. 4 Typical OCT image of leaf sample from virus-free but stressed plants. Scale bar corresponds to 100 μm.

3.2 *Histological Analysis*

In this section, we investigate whether the highly scattering feature observed in the epidermal layer of virus-infected leaf samples is visible under bright-field histological observation. Histological sections of healthy and virus-infected leaf samples were examined. Figures 5(a) and 5(b) show the typical histological cross sections of healthy and virus-infected leaves, respectively. Morphological features such as the epidermal layers and vascular bundles are observed to be similar in appearance between the healthy and virus-infected samples. Although the bright-field images showed considerable details of cellular structures, there appears to be no discernible difference between the histological images of healthy and virus-infected samples. In particular, the highly scattering epidermal layers seen in the OCT images of virus-infected samples are not observed in the corresponding histological sections. One possible explanation is that the content within the leaf cells is altered or removed by the histological preparation process. To examine the plant cells in their original form, cryosections of the leaf samples were also taken without any fixation or staining. These cryosections were then mounted on microscope slides and observed under both bright-field and phase-contrast microscopes. We were also unable to observe any epidermal differences between the cryosections of healthy and virus-infected leaf samples.

4 Discussion

The OCT images of Oncidium orchid leaves revealed a characteristic highly scattering epidermal layer when the plant was infected with CymMV. The significant increase in scattering in the epidermis of the virus-infected samples may be associated with cell death processes such as autophagy, which plays a protective role against external infection.[19] The autophagy process involves the degradation or breakdown of intracellular components,[20] which can give rise to the changes in the optical scattering characteristics of the epidermal cells by increasing their overall scattering cross sections. In particular,

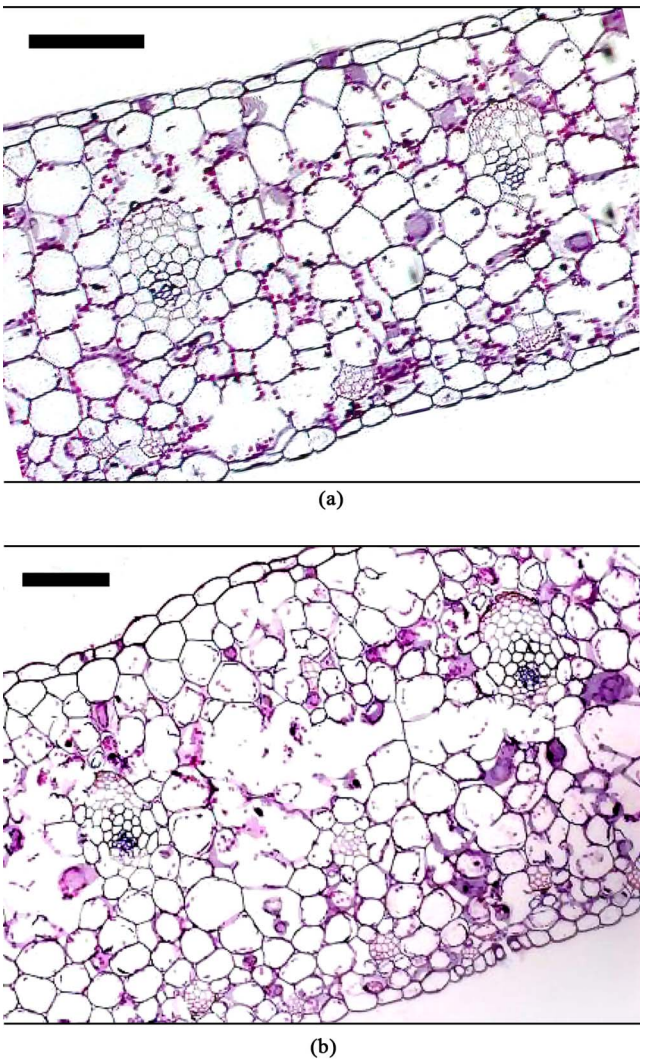

Fig. 5 Histological sections of (a) healthy and (b) virus-infected leaf samples. Scale bar corresponds to 100 μm.

OCT imaging has shown the capability to pick out early degradation before obvious visible symptoms can be observed. This corroborates previous work that showed that the increase of autolysosomes due to the autophagy process can lead to an increase in the scattering characteristics.[19] The reason for the general lack of significant scattering signals from the intracellular region of mesophyll cells in virus-infected leaf samples is unknown and is a subject of future study.

The highly scattering feature in the epidermal layers of virus-infected leaf samples was not observed in the leaves of stressed plants, despite showing similar visual symptoms as virus-infected plants. This suggests that the highly scattering feature in the epidermis is related to the CymMV infection and can be used to accurately identify virus-infected orchid plants. Histological analysis of the leaf samples showed that the highly scattering feature in virus-infected samples cannot be observed under bright-field microscopic observation. This is possibly due to the relatively low scattering coefficients of plant tissues[18] and the small difference between the scattering coefficients of healthy and virus-infected epidermal tissues. By contrast, the high sensitivity of OCT ensures that subtle differences in the scattering properties of the epidermal layers can be detected.

It has been reported that plant viruses have different degrees of infection for different orchids,[21] thereby leading to different responses by the plants to the viruses. In view of this, plants may not experience autophagy or changes in tissue morphology when virus infection is low, thus limiting the effectiveness of OCT imaging. This necessitates the need for further work to quantify the responses of other orchids to various viruses with OCT imaging. Optical characteristics such as scattering coefficients of the plant tissue can provide a quantitative measure of the degradation of the plant, and thereby infer the dominant virus type in the plant. For instance, viruses that trigger stronger hypersensitive responses (HR) may in general have higher scattering contrast compared to one that has lower HR. Studies have also shown that the roots of orchids generally have the *highest* uptake of virus when an infection occurs.[15] The possibility of imaging the root instead of the leaves may also improve the effectiveness of diagnosing the health of the plant.

Besides giving the optical cross sectional images of orchid leaves, this work shows that OCT can detect a distinctive highly scattering epidermal layer in the leaves of virus-infected plants. This highly scattering feature can be used to quickly diagnose virus infection in orchid plants by imaging their leaves with an OCT system. The OCT system can be made portable and compact by replacing the femtosecond laser used in this work with a broadband superluminescent diode (SLD) source.[22] Real-time OCT imaging can be achieved through the use of fast charge-coupled device (CCD) arrays.[12] A probe-based sample arm in the OCT system will allow *in-situ* diagnosis of the orchid plants. Such a tool will enable orchid growers and import authorities to carry out nondestructive, real-time screening of orchid plants for virus infection.

5 Conclusion

We investigate the use of OCT for diagnosing virus infection in orchid plants. The morphological structure of cells within the orchid leaves can clearly be seen in the high resolution OCT images. Highly scattering upper and lower epidermal layers in the leaves of virus-infected plants, which are not visible under histological observation, are detected with the OCT technique. This highly scattering feature is not present in the leaf epidermides of stressed but healthy plants, which can exhibit similar visual symptoms as virus-infected plants. Consequently virus-infected orchid plants can be accurately identified by imaging the epidermal layer of their leaves with OCT. The OCT modality is found to be suitable for fast, nondestructive diagnosis of orchid virus infection, which can potentially lead to significant cost savings and better control of the spread of viruses in the orchid industry.

Acknowledgments

We acknowledge the technical assistance of Siu-Ling Ho, Woon-Li Wen, and Swee-Hoon Koe for the preparation of the histological slides. This research was supported in part by a

research grant from the Singapore Cancer Syndicate (SCS-BU0052) under the Agency for Science, Technology and Research (A*STAR).

References

1. L. T. Lam-Chan, B. L. pohl, and F. Suhaimi, "Annual floriculture trade 2006," *Plant Bulletin* **1**, 1–2 (2007).
2. S. M. Wong, C. G. Ching, Y. H. Lee, K. Tan, and F. W. Zettler, "Incidence of cymbidium mosaic and odontoglossum ringspot viruses and their significance in orchid cultivation in Singapore," *Crop Protection* **13**(3), 235–239 (1994).
3. R. Vejaratpimol, C. Channuntapipat, P. Liewsaree, T. Pewnim, K. Ito, M. Iizuka, and N. Minamiura, "Evaluation of enzyme-linked immunosorbent assays for the detection of cymbidium mosaic virus in orchids," *J. Ferment. Bioeng.* **86**(1), 65–71 (1998).
4. S. T. Lim, S. M. Wong, C. Y. Yeong, S. C. Lee, and C. J. Goh, "Rapid detection of cymbidium mosaic virus by the polymerase chain reaction (PCR)," *J. Virol. Methods* **41**(1), 37–46 (1993).
5. W. Drexler, U. Morgner, R. K. Ghanta, F. X. Kartner, J. S. Schuman, and J. G. Fujimoto, "Ultrahigh-resolution ophthalmic optical coherence tomography," *Nat. Med.* **7**(4), 502–506 (2001).
6. D. Huang, E. A. Swanson, C. P. Lin, J. S. Schuman, W. G. Stinson, W. Chang, M. R. Hee, T. Flotte, K. Gregory, C. A. Puliafito, and J. G. Fujimoto, "Optical coherence tomography," *Science* **254**(5035), 1178–1181 (1991).
7. T. Gambichler, G. Moussa, M. Sand, D. Sand, P. Altmeyer, and K. Hoffmann, "Applications of optical coherence tomography in dermatology," *J. Dermatol. Sci.* **40**(2), 85–94 (2005).
8. J. G. Fujimoto, M. E. Brezinski, G. J. Tearney, S. A. Boppart, B. Bouma, M. R. Hee, J. F. Southern, and E. A. Swanson, "Optical biopsy and imaging using optical coherence tomography," *Nat. Med.* **1**(9), 970–972 (1995).
9. J. W. Hettinger, M. D. P. Mattozzi, W. R. Myers, M. E. Williams, A. Reeves, R. L. Parsons, R. C. Haskell, D. C. Petersen, R. Y. Wang, and J. I. Medford, "Optical coherence microscopy. A technology for rapid, in vivo, non-destructive visualization of plants and plant cells," *Plant Physiol.* **123**(1), 3–15 (2000).
10. A. Reeves, R. L. Parsons, J. W. Hettinger, and J. I. Medford, "In vivo three-dimensional imaging of plants with optical coherence microscopy," *J. Microsc.* **208**(3), 177–189 (2002).
11. M. Boccara, W. Schwartz, E. Guiot, G. Vidal, R. De Paepe, A. Dubois, and A. C. Boccara, "Early chloroplastic alterations analysed by optical coherence tomography during a harpin-induced hypersensitive response," *Plant J.* **50**(2), 338–346 (2007).
12. R. A. Leitgeb, W. Drexler, A. Unterhuber, B. Hermann, T. Bajraszewski, T. Le, A. Stingl, and A. F. Fercher, "Ultrahigh resolution Fourier domain optical coherence tomography," *Opt. Express* **12**(10), 2156–2165 (2004).
13. P. C. Cheng, B. L. Lin, F. J. Kao, M. Gu, M. G. Xu, X. Gan, M. K. Huang, and Y. S. Wang, "Multi-photon fluorescence microscopy-The response of plant cells to high intensity illumination," *Micron* **32**(7), 661–669 (2001).
14. T. F. Chia, Y. S. Chan, and N. H. Chua, "Characterization of cymbidium mosaic virus coat protein gene and its expression in transgenic tobacco plants," *Plant Mol. Biol.* **18**(6), 1091–1099 (1992).
15. T. F. Chia, Y. S. Chan, and N. H. Chua, "Detection and localization of viruses in orchids by tissue-print hybridization," *Plant Pathol.* **41**(3), 355–361 (1992).
16. T. F. Chia and J. He, "Photosynthetic capacity in Oncidium (Orchidaceae) plants after virus eradication," *Environ. Experimental Botany* **42**(1), 11–16 (1999).
17. M. Seyfried, L. Fukshansky, and E. Schafer, "Correcting remission and transmission spectra of plant tissue measured in glass cuvettes: a technique," *Appl. Opt.* **22**(3), 492–496 (1983).
18. H. W. Gausman and W. A. Allen, "Optical parameters of leaves of 30 plant species," *Plant Physiol.* **52**, 57–62 (1973).
19. Y. Liu, M. Schiff, K. Czymmek, Z. Tallóczy, B. Levine, and S. P. Dinesh-Kumar, "Autophagy regulates programmed cell death during the plant innate immune response," *Cell* **121**(4), 567–577 (2005).
20. J. T. Greenberg, "Degrade or die: A dual function for autophagy in the plant immune response," *Dev. Cell* **8**(6), 799–801 (2005).
21. J. S. Hu, S. Ferreira, M. Wang, and M. Q. Xu, "Detection of Cymbidium Mosaic-Virus, Odontoglossum Ringspot Virus, Tomato Spotted Wilt Virus, and Potyviruses Infecting Orchids in Hawaii," *Plant Dis.* **77**(5), 464–468 (1993).
22. T. H. Ko, D. C. Adler, J. G. Fujimoto, D. Mamedov, V. Prokhorov, V. Shidlovski, and S. Yakubovich, "Ultrahigh resolution optical coherence tomography imaging with a broadband superluminescent diode light source," *Opt. Express* **12**(10), 2112–2119 (2004).